

Faster-HEAL: An Efficient and Privacy-Preserving Collaborative Perception Framework for Heterogeneous Autonomous Vehicles

Armin Maleki

*Electrical and Computer Engineering
Michigan State University
East Lansing, Michigan
malekiar@msu.edu*

Hayder Radha

*Electrical and Computer Engineering
Michigan State University
East Lansing, Michigan
radha@msu.edu*

Abstract—Collaborative perception (CP) is a promising paradigm for improving situational awareness in autonomous vehicles by overcoming the limitations of single-agent perception. However, most existing approaches assume homogeneous agents, which restricts their applicability in real-world scenarios where vehicles use diverse sensors and perception models. This heterogeneity introduces a feature domain gap that degrades detection performance. Prior works address this issue by retraining entire models/major components, or using feature interpreters for each new agent type, which is computationally expensive, compromises privacy, and may reduce single-agent accuracy. We propose Faster-HEAL, a lightweight and privacy-preserving CP framework that fine-tunes a low-rank visual prompt to align heterogeneous features with a unified feature space while leveraging pyramid fusion for robust feature aggregation. This approach reduces the trainable parameters by 94%, enabling efficient adaptation to new agents without retraining large models. Experiments on the OPV2V-H dataset show that FASTER-HEAL improves detection performance by 2% over state-of-the-art methods with significantly lower computational overhead, offering a practical solution for scalable heterogeneous CP.

Index Terms—Autonomous Vehicles, Collaborative Perception, Heterogeneous Fusion, Visual Prompts, Privacy-Preserving

I. INTRODUCTION

With the growing deployment of autonomous vehicles, ensuring reliable and safe operation is critical. Collaborative perception (CP) has emerged as a key paradigm to enhance situational awareness in connected autonomous vehicles (CAVs) by sharing perception information, giving agents a more complete view of occluded and long-range regions and improving safety and accuracy [1]. Despite growing interest, collaborative perception still faces bandwidth limits, communication latency, sensor noise, and pose estimation errors, which can severely degrade system performance. While recent work has made progress in mitigating bandwidth, latency, and pose issues [2]–[6], most methods assumed homogeneous sensors and identical perception models across vehicles, which simplifies design and limits applicability in real-world deployments. In practice, vehicles from different manufacturers use diverse sensor configurations and perception networks, creating a feature domain gap between agents. This heterogeneity can degrade downstream

perception performance and safety; hence, bridging this gap is essential for robust, safety-critical collaborative perception in real-world autonomous driving.

Prior work on heterogeneous collaborative perception falls into two main approaches. The first closes the domain gap by retraining parts of the ego or neighbor models to project features into a unified feature space [7], [8], [10], [11]. Specifically, HETerogeneous ALliance (HEAL) [11] uses two stages: first, the ego and *homogeneous agents* are trained with a standard collaborative perception strategy to build a unified feature space, and then each new heterogeneous agent retrains its encoder and other modules to map its inputs into that space. This approach is effective but impractical, since every new agent type must be retrained, which is costly for real-time deployment and can harm both privacy and single-agent performance. Because some vehicles’ model/sensor stacks are proprietary, sharing parameters or retraining on private data is often not feasible. The second approach introduces feature interpreters that translate or align heterogeneous features to the unified feature space, preserving single-agent performance and model confidentiality [12]–[14]. However, these interpreters usually rely on larger, more expensive models and still need retraining or extra storage whenever a new heterogeneous agent joins. These limitations motivate methods that generalize efficiently to unseen agents while maintaining accuracy, privacy, and computational feasibility.

In this paper, we propose **Faster-HEAL**, a heterogeneous collaborative perception framework that efficiently bridges the semantic domain gap between heterogeneous agents while preserving privacy and improving computational efficiency over HEAL [11]. Building on the first stage of HEAL, we introduce a novel **Lightweight Interpreter for Feature Transformation (LIFT)** that aligns intermediate features from new heterogeneous neighbor agents with the ego agent’s unified feature space. The framework is trained in two stages: first, the ego agent is trained on a homogeneous CP base to construct the unified feature space and fusion model; second, LIFT is fine-tuned to map new heterogeneous agents’ features into that space along with two other small components. This

design preserves the privacy and single-agent accuracy of new agents, avoids costly retraining and storage overhead, and enables scalable deployment. By combining the unified feature space with LIFT, FASTER-HEAL mitigates performance degradation in heterogeneous settings while maintaining high computational efficiency, and preserving privacy.

We leverage visual prompts as the core mechanism in our LIFT-based feature interpreter, which guides the model by emphasizing task-relevant information in the feature representation, like language prompts. Since visual prompts have high dimensionality, naively training them is computationally expensive. We therefore design a low-rank prompt representation that reduces the number of trainable parameters by an order of magnitude and significantly improves training efficiency.

Our key contributions are summarized as follows:

- We design **Faster-HEAL**, which uses a lightweight interpreter for feature translation (**LIFT**) for newly emerging heterogeneous agent types, enabling single-stage feature alignment with the ego agent’s unified feature space. For each new agent type with a different modality, only a visual prompt is fine-tuned along with a feature aligner, so the ego agent needs only intermediate features, and each vehicle keeps sensor/model configurations private.
- By introducing low-rank visual prompts as LIFT, our approach achieves fast and accurate feature adaptation while reducing trainable parameters and computation by an order of magnitude, and lowering storage overhead, since only the LIFT for different agent types are stored.
- Experimental results show that FASTER-HEAL improves state-of-the-art detection performance by 2% while reducing computational overhead by 94% on average for training, representing a practical step toward scalable and privacy-preserving CP in real-world autonomous driving.

II. RELATED WORK

A. Collaborative Perception

Sharing perception data among connected agents through collaborative perception improves the accuracy and reliability of downstream tasks, especially in occluded or long-range scenarios. CP is usually categorized into three levels based on the granularity of shared and fused information [1]: (a) early fusion, which transmits raw sensor data and can maximize perception performance but requires very high bandwidth; (b) late fusion, which exchanges only final detection results, saving bandwidth but suffering from noise accumulation and inconsistent predictions; (c) intermediate fusion, which shares processed feature representations to balance communication efficiency and perception quality. Recent intermediate-fusion methods such as Where2com [2] and Codefilling [5] dynamically select communication partners, timing, or content to relieve bandwidth pressure while preserving performance. Other studies further tackle noisy communication, latency, and pose estimation errors that misalign shared features [3], [4], [6]. However, most existing frameworks still assume homogeneous sensors and perception models across agents, leaving heterogeneity as a key open challenge.

B. Heterogeneous Collaborative Perception

Addressing the performance degradation caused by the feature domain gap among heterogeneous agents has become an active research area. Most approaches mitigate this gap by retraining the whole network or part of it to align features across agents. DI-V2X [7], HM-ViT [8], DGCNN [9], and CoCMT [10] each address the domain gap for each agent type by retraining the model or selected submodules, which increases computational overhead, violates neighbors’ privacy, and adapts poorly to new agent types at deployment. HEAL [11] further proposes a pyramid fusion model that builds a unified feature space but still requires retraining the new agent’s encoder, again raising data privacy concerns. To avoid modifying full perception stacks, MDPA [12] and PnPDA+ [13] use feature interpreters to align new-agent features to a unified feature space, reducing the amount of retraining while keeping the original perception models intact. Specifically, PolyInter [14] adopts visual prompts alongside attention modules as interpreters. These approaches limit retraining to a dedicated module, but they often incur higher model complexity and computational overhead.

C. Visual Prompts

Prompt-based learning has recently emerged as a powerful tool for domain adaptation in vision tasks, enabling models to bridge feature distribution gaps with minimal parameter updates. By injecting learnable visual tokens into the feature space, visual prompts guide the network to adapt to new domains and improve downstream task performance without full model retraining. AD-CLIP [15], ViP-LLaVA [16], and UPRE [18] use visual prompts to mitigate domain gaps for classification by learning domain-invariant features. In contrast, DPR [17] and ModPrompt [19] address detection performance degradation under heterogeneous features via visual prompt tuning. Collectively, these works establish visual prompts as a compact mechanism for domain alignment, offering strong performance gains with minimal computation.

III. METHODOLOGY

The overall architecture of FASTER-HEAL is shown in Fig. 1. The framework has two stages to address feature misalignment in heterogeneous collaborative perception. In stage 1, we adopt the homogeneous base training architecture and loss of HEAL [11], to learn a unified feature space for the ego agent. A brief summary appears in Subsection III-A. In stage 2, we introduce and fine-tune **LIFT** as lightweight visual prompts to align the newly introduced heterogeneous intermediate features with the ego agent unified space, enabling rapid adaptation (to the best of our knowledge, among the lowest interpreter-based methods) while preserving privacy and single-agent performance (unlike retraining methods).

A. Homogeneous Base Training

In the first stage of FASTER-HEAL, we learn a unified feature space using the ego agent (e) and $N - 1$ homogeneous neighbors. For each agent $i \in \{1, 2, \dots, N-1, N\}$ (N is for e),

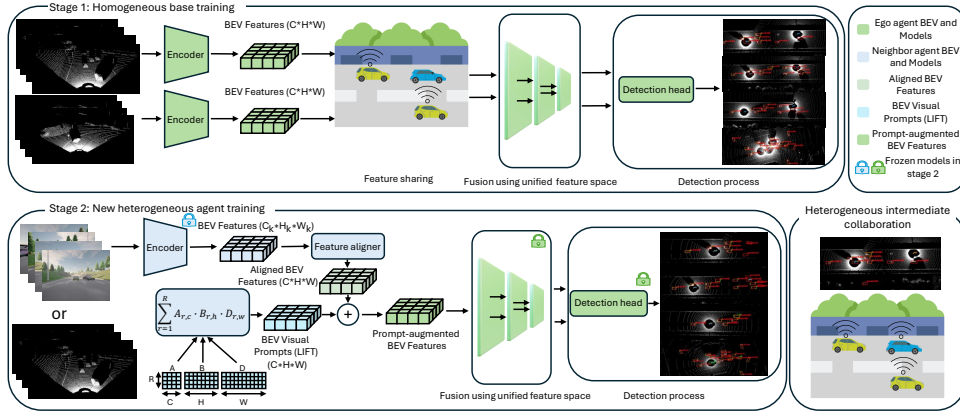


Fig. 1. Overview of **FASTER-HEAL**. Stage 1: Homogeneous base training constructs a unified feature space using pyramid fusion and trains the detection head on collaborative data from homogeneous agents. stage 2: For each new heterogeneous agent type, we freeze the pretrained encoder, pyramid fusion extractor/upsampling path, and detection head, and train a lightweight feature aligner, LIFT (visual prompts) to map its intermediate features into the unified space, and the foreground estimator. This design ensures low training cost, preserves the privacy of participating agents by requiring only their intermediate features, and enables scalable heterogeneous collaboration. In our experiments, LiDAR is used in stage 1, while camera or LiDAR could be used in stage 2.

the observation O_i is encoded by the shared ego encoder f_{enc_ego} into BEV features F_i , which are transformed to the ego frame and transmitted as $F_{i \rightarrow e}$ via communication function $\Gamma_{i \rightarrow e}$. The ego then fuses all received features $\{F_{i \rightarrow e}\}$ using the pyramid fusion module $f_{pyramid}$ to obtain the ego agent unified fused representation H_e , which is passed to the detection head f_{head} to produce the final detections B :

$$\begin{aligned}
 F_i &= f_{enc_ego}(O_i), i = 1, 2, \dots, N \\
 F_{i \rightarrow e} &= \Gamma_{i \rightarrow e}(F_i), i = 1, 2, \dots, N \\
 H_e &= f_{pyramid}(F_{1 \rightarrow e}, F_{2 \rightarrow e}, \dots, F_{N \rightarrow e}) \\
 B &= f_{head}(H_e)
 \end{aligned} \tag{1}$$

To enable efficient and accurate feature fusion, we adopt the Pyramid Fusion module from [11]. A ResNeXt network [20] progressively downsamples incoming features by factor of two, producing L multi-scale features. At each scale l , a foreground estimator generates an occupancy map that is normalized across agents to obtain fusion weights. The weighted features are then aggregated, upsampled to a common resolution, and concatenated to form fused features H_e :

$$\begin{aligned}
 F_{i \rightarrow e}^{(l)} &= f_{ResNeXt}^{(l)}(F_{i \rightarrow e}^{(l-1)}), i = 1, 2, \dots, N, l = 1, \dots, L \\
 OCC_{i \rightarrow e}^{(l)} &= f_{foreground}^{(l)}(F_{i \rightarrow e}^{(l)}), i = 1, 2, \dots, N, l = 1, \dots, L \\
 W_{i \rightarrow e}^{(l)} &= \text{softmax}(OCC_{1 \rightarrow e}^{(l)}, \dots, OCC_{N \rightarrow e}^{(l)}), \\
 F_e^{(l)} &= \sum_{i=1}^N F_{i \rightarrow e}^{(l)} \cdot W_{i \rightarrow e}^{(l)}, \\
 F_e^{(l)} &= f_{upsample}^{(l)}(F_e^{(l)}), l = 1, \dots, L \\
 H_e &= \text{concat}(F_e^{(1)}, F_e^{(2)}, \dots, F_e^{(L)}),
 \end{aligned} \tag{2}$$

where l denotes the scale level, and $f_*^{(l)}$ indicates the corresponding ResNeXt, upsampling, or foreground estimation.

Using multi-scale features in the unified feature space leverages coarse-to-fine features, improving fusion adaptivity

and robustness to transformation errors, while the foreground estimator focuses on informative regions of each agent's feature map to enhance downstream detection.

The total training loss for the homogeneous base stage is the sum of the final detection loss and the supervised foreground estimation losses at all scales:

$$\begin{aligned}
 L &= L_{det}(B, Y) + \sum_{l=1}^L \alpha_l L_{foreground}^{(l)} \\
 L_{det}(B, Y) &= L_{focal}(B, Y) \\
 &+ 2 \cdot L_{smooth-L1}(B, Y) + 0.2 \cdot L_{dir}(B, Y) \\
 L_{foreground}^{(l)} &= \sum_{i=1}^N L_{focal}(OCC_{i \rightarrow e}^{(l)}, Y_{i \rightarrow e}^{(l)}),
 \end{aligned} \tag{3}$$

where, L_{focal} , $L_{smooth-L1}$, and L_{dir} denote the focal classification loss, regression loss, and direction loss, respectively; Y and B are the ground-truth and predicted detections. At each scale l , the foreground estimator is supervised by focal loss on the predicted occupancy map and its BEV mask $Y_{i \rightarrow e}^{(l)}$, with α_l weighting the contribution of each scale.

B. New heterogeneous agent training

After training the homogeneous base, new heterogeneous agents may join the collaboration group. The BEV feature domain gap caused by different sensors, perception models, or sensor configurations can significantly degrade performance, so the ego agent cannot directly use their raw intermediate features and must first align them with its unified feature space. In real-world deployments, computational and time resources are limited, and retraining the new agent's model is often infeasible, while manufacturers are typically unwilling to share parameters or modify proprietary networks. These constraints motivate a lightweight, privacy-preserving mechanism to adapt heterogeneous features efficiently.

The key idea of FASTER-HEAL in this stage is to adapt features from newly introduced heterogeneous agents while

preserving the ego agent’s unified feature space. We freeze the ego fusion extractor/upsampling and detection modules as well as the new agent’s encoder, so the learned representation stays consistent, and only intermediate features are shared, which preserves the new agent’s privacy by avoiding access to its sensor configurations or model parameters, unlike HEAL [11].

To close the domain gap, FASTER-HEAL injects learnable visual prompts as LIFT to the transmitted intermediate features, fine-tuning a separate prompt for each new agent type to make its representation compatible with the ego agent’s unified feature space. For a new agent k of type n_1 with observation O_k and frozen encoder $f_{enc_{n_1}}$, the second-stage training is:

$$\begin{aligned} F_k &= f_{enc_{n_1}}^{**}(O_k), \\ F_{k \rightarrow e} &= \Gamma_{k \rightarrow e}(F_k), \\ F'_k &= f_{aligner_{n_1}}(F_{k \rightarrow e}), \\ F''_k &= F'_k + P_{n_1}, \\ H_{e,k} &= f_{pyramid}^*(F''_k), \\ B_k &= f_{head}^*(H_{e,k}), \end{aligned} \quad (4)$$

where F_k is the intermediate BEV feature of agent k , $F_{k \rightarrow e}$ is its spatially transformed feature, and F'_k is the channel-aligned output of the aligner $f_{aligner_{n_1}}$, which employs a ConvNeXt-based [21] projection that maps (C_k, H_k, W_k) to (C, H, W) . P_{n_1} is the learnable visual prompt for agent type n_1 , F''_k is the prompt-augmented feature fed to the frozen pyramid fusion module, $H_{e,k}$ is agent k ’s features in the ego unified representation, and B_k is the final detection. The superscript $*$ (from stage 1), $**$ (from neighbor) indicates the corresponding module is pretrained and kept frozen in this stage.

To ensure compatibility, the visual prompt P_{n_1} has the same channels, height, and width (C, H, W) as the aligned neighbor features, which match the ego features. P_{n_1} is randomly initialized and fine-tuned using the ground-truth detection loss. However, even a small BEV prompt contains $C \times H \times W$ trainable parameters, which may exceed the size of a typical encoder and lead to high computational cost and slow convergence. To address this challenge, FASTER-HEAL applies PARAFAC decomposition [29] to factorize the prompt into a low-rank representation. Let R denote the decomposition rank; three 2D tensors are initialized as $A \in \mathbb{R}^{R \times C}$, $B \in \mathbb{R}^{R \times H}$, and $D \in \mathbb{R}^{R \times W}$, where C , H , and W are the channel, and spatial dimensions. The prompt is then reconstructed as

$$P_{c,h,w} \approx \sum_{r=1}^R A_{r,c} \cdot B_{r,h} \cdot D_{r,w}, \quad (5)$$

where $P_{c,h,w}$ is the prompt element at channel c and spatial location (h, w) . This factorization reduces the trainable parameters from $C \times H \times W$ to $R \times (C + H + W)$ with $R \ll \min(C, H, W)$, shrinking them from millions to a few thousand, which lowers training cost, speeds convergence, and, retains performance comparable to full-prompt tuning at a fraction of the computational overhead.

Training the aligner primarily resolves dimensional/statistical mismatch, while LIFT (visual prompts)

ensures effective feature alignment and robust multi-scale domain adaptation, and retraining the foreground estimator for new agents emphasizes domain-specific salient regions and improves fusion quality. By freezing the encoders of new agents, FASTER-HEAL preserves privacy by avoiding any sharing of model weights or sensor parameters, and centralized training at the ego side removes the need to retrain other agents. This design also reduces storage, since only compact LIFT (prompt parameters) are stored instead of full encoder models for each agent type. Once stage 2 is completed for heterogeneous types n_1, n_2, \dots , the ego agent can collaborate with any agent of these types, and the prompt-based adaptation can be further retrained if needed, enhancing the robustness and scalability of the collaborative perception framework. The loss function used in this stage is identical to that of the first training stage, combining detection loss and supervised foreground losses across scales.

C. Inference Implementation

After completing stage 2 training for a heterogeneous neighbor, the ego agent shares the trained aligner with that neighbor to enable collaborative perception. The aligner compresses the neighbor’s intermediate features before transmission, reducing communication bandwidth, while privacy is preserved since no agent shares its full model or sensor specifications. At deployment, each agent includes a type-ID (e.g., sensor and encoder modality). Then the ego uses this ID to select the matching {aligner, LIFT} pair, without needing access to proprietary sensor or model parameters, and shares the matching aligner. If the new agent’s model parameters differ from those seen during stage 2, a slight performance degradation may occur, but the system remains functional. If desired, the ego can fine-tune the LIFT for a few epochs to better adapt to this agent. Due to the domain similarity between models of the same type and the very small number of trainable prompt parameters (fewer than 10k), this adaptation can be performed rapidly, approaching real-time performance.

IV. EXPERIMENTS

A. Datasets

We evaluate FASTER-HEAL on OPV2V-H dataset to assess its performance. OPV2V-H [11] is a public dataset built upon OPV2V [22], a large-scale benchmark for collaborative perception in autonomous driving.

B. Scenario Design

To evaluate the generalization capability of FASTER-HEAL across different sensor types and perception encoders, we design scenarios with both LiDAR- and camera-based agents. For LiDAR, we adopt *PointPillar* [23] and *SECOND* [24] as feature encoders. For camera-based agents, we use *EfficientNet* [25] and *ResNet-50* [26] as image encoders in conjunction with *Lift-Splat-Shoot* [27] for BEV feature generation.

To ensure comparability with prior work, we follow the HEAL [11] framework and train the homogeneous base using a 64-channel LiDAR agent (m_1) with PointPillar to construct the

unified feature space. For heterogeneous experiments, we add three new agent types: (i) a camera-based agent with EfficientNet (m_2), (ii) a LiDAR agent using SECOND (m_3), and (iii) a camera-based agent with ResNet-50 (m_4). All LiDAR and camera encoders use a BEV grid resolution of $[0.4\text{ m}, 0.4\text{ m}]$, and their encoded features pass through a BEV backbone before fusion. The aligner uses a ConvNeXt [21] projection to match feature size to the ego space, and the pyramid fusion module operates over three scales with $[64, 128, 256]$ and $[3, 5, 8]$ ResNeXt [20] blocks, and 1×1 foreground estimator at each scale. All new agents use pretrained and frozen single-agent encoders and BEV backbones to avoid retraining large models. Both the base training stages run for 25 epochs with Adam (learning rate 0.002). The detection range is $[-102.4\text{ m}, +102.4\text{ m}]$ along x and $[-51.2\text{ m}, +51.2\text{ m}]$ along y . We evaluate average precision (AP) at different intersection-over-union (IoU) thresholds and, during testing, initialize each scenario with the base agent and then progressively introduce new heterogeneous agent types to assess adaptability.

C. Results

We compare FASTER-HEAL with state-of-the-art intermediate fusion frameworks for heterogeneous collaborative perception. As summarized in Table I, FASTER-HEAL improves HEAL [11] by about 1.8%/1.3% at AP@0.5/0.7 IoU and outperforms CoBEVT [28] by 5.3%/12% at AP@0.5/0.7, showing that fine-tuning LIFT is an effective way to handle sensor and model heterogeneity of new agents without retraining the whole or a part of the perception stacks. The last three columns of Table I report the number of trainable parameters where FASTER-HEAL reduces them from tens of millions (as in HEAL and other retraining-based approaches) to only a few hundred thousand, a reduction of roughly 90%, while improving accuracy, makes FASTER-HEAL practical for real-world deployments, where fast adaptation and low storage overhead are crucial. Training efficiency in Table II further shows that FASTER-HEAL reaches 16.64 TFLOPs/s, about $2.35 \times$ higher hardware utilization and $1.2 \times$ higher end-to-end training throughput than HEAL, while lowering peak GPU memory by 38% on an NVIDIA RTX A6000 with batch size 1, confirming FASTER-HEAL is both accurate and computationally efficient.

D. Ablation Study

We analyze the contribution of each trainable component in stage 2 of FASTER-HEAL. We fix the decomposition rank at $R = 8$ and compare freezing versus fine-tuning the encoder, BEV backbone, and LIFT. As shown in Table III, fine-tuning only the LIFT yields the largest performance gain, most effectively addressing the domain gap, and uses only 340k parameters. In contrast, retraining the encoder or BEV backbone alongside LIFT brings no extra benefits and instead causes overfitting and slower convergence. This confirms that lightweight prompt fine-tuning offers the best accuracy–efficiency trade-off and validates our design choice.

We further evaluate the effect of the PARAFAC decomposition rank R on model performance. As in Eq. 5, each prompt element P is reconstructed by summing over R . Hence, the number of trainable parameters varies with R (varies 3%-9%), while its impact on training speed is negligible. For fairness, we fix all other configurations and vary only R . Table IV shows that $R = 8$ provides the best performance–efficiency trade-off, where $R = 4$ underfits, and $R = 16$ and $R = 32$ lead to overfitting and slower convergence.

V. CONCLUSION

In this paper, we introduced **Faster-HEAL**, a novel framework for open heterogeneous collaborative perception that fine-tunes lightweight visual prompts (**LIFT**) in a unified feature space. Our method achieves state-of-the-art detection performance with only a fraction of the trainable parameters of prior methods, preserving computational efficiency and privacy, since training relies solely on shared intermediate features and does not require access to internal architectures or model parameters of the new agent. Experiments on OPV2V-H demonstrate that FASTER-HEAL mitigates the feature domain gap caused by heterogeneous sensors/models effectively, enabling fast adaptation without retraining entire perception stacks and representing a practical, scalable privacy-preserving CP framework in real-world autonomous driving. Extending the evaluation to additional CP datasets/baselines, and more diverse sensor/model/noise configurations, is left for the future. **Acknowledgment** This work was supported by a Department of Transportation/Federal Railroad Administration grant.

REFERENCES

- [1] T. Huang, J. Liu, X. Zhou, D. C. Nguyen, M. R. Azghadi, Y. Xia, Q. L. Han, and S. Sun, V2X cooperative perception for autonomous driving: Recent advances and challenges. arXiv preprint arXiv:2310.03525, 2023.
- [2] Y. Hu, S. Fang, Z. Lei, Y. Zhong, S. Chen, Where2comm: Communication-efficient collaborative perception via spatial confidence maps. Advances in neural information processing systems, 2022.
- [3] Z. Lei, S. Ren, Y. Hu, W. Zhang, and S. Chen, Latency-aware collaborative perception. In Computer Vision–ECCV 2022: 17th European Conference, 2022.
- [4] Y. Lu, Q. Li, B. Liu, M. Dianat, C. Feng, S. Chen, and Y. Wang, “Robust collaborative 3D object detection in presence of pose errors,” in Proceedings of the IEEE International Conference on Robotics and Automation (ICRA), London, United Kingdom, 2023, pp. 4812–4818.
- [5] Y. Hu, J. Peng, S. Liu, J. Ge, S. Liu, and S. Chen, Communication-efficient collaborative perception via information filling with codebook. In Proceedings of the IEEE/CVF Conference on Computer Vision and Pattern Recognition (CVPR), pages 15481–15490, 2024.
- [6] S. Su, Y. Li, S. He, S. Han, C. Feng, C. Ding, and F. Miao, “Uncertainty quantification of collaborative detection for self-driving,” in Proceedings of the IEEE International Conference on Robotics and Automation (ICRA), London, UK, 2023, pp. 5588–5594.
- [7] X. Li, J. Yin, W. Li, C. Xu, R. Yang, and J. Shen, “Di-v2x: Learning domain-invariant representation for vehicle-infrastructure collaborative 3d object detection,” in Proceedings of the AAAI Conference on Artificial Intelligence, vol. 38, n. 4, 2024, pp. 3208–3215.
- [8] H. Xiang, R. Xu, and J. Ma, “HM-ViT: Hetero-modal vehicle-to-vehicle cooperative perception with vision transformer,” in Proceedings of the IEEE/CVF International Conference on Computer Vision (ICCV), Paris, France, 2023, pp. 284–295.
- [9] P. Zhi, L. Jiang, X. Yang, X. Wang, H. W. Li, Q. Zhou, et al., Cross-domain generalization for lidar-based 3d object detection in infrastructure and vehicle environments. Sensors. January 2025.

TABLE I

DETECTION PERFORMANCE COMPARISON ON OPV2V-H USING m_1 AS THE COLLABORATIVE BASE AND PROGRESSIVELY ADDING THREE NEW HETEROGENEOUS AGENTS (m_2, m_3, m_4). WE REPORT AP@0.5, AP@0.7, AND THE MODEL NUMBER OF TRAINABLE PARAMETERS FOR NO-FUSION, LATE FUSION (NO RETRAINING), HEAL [11] (ENCODER RETRAINING), AND COBEVT [28] THAT RETRAIN THEIR ENTIRE MODEL.

Metric	AP@0.5(%) \uparrow			AP@0.7(%) \uparrow			Model #Training Params (M) \downarrow		
	$+m_2$	$+m_3$	$+m_4$	$+m_2$	$+m_3$	$+m_4$	$+m_2$	$+m_3$	$+m_4$
Based on m_1, Add New Agent									
No Fusion	74.8	74.8	74.8	60.6	60.6	60.6	/	/	/
Late Fusion	77.5	83.3	83.4	59.9	68.5	68.5	/	/	/
CoBEVT [28]	82.2	88.5	88.5	67.1	74.2	74.2	33.24	42.05	51.68
HEAL (reported by [11])	82.6	89.2	89.4	72.6	81.2	81.3	15.01	1.08	1.91
HEAL (trained with ours configurations)	87.2	91.3	90.9	78.3	84.8	84.5	15.01	1.08	1.91
FASTER-HEAL (ours)	89.3	93.0	92.7	79.7	86.3	85.7	0.113	0.113	0.113
Improvement w.r. to HEAL	$\uparrow 2.1$	$\uparrow 1.7$	$\uparrow 1.8$	$\uparrow 1.4$	$\uparrow 1.5$	$\uparrow 1.2$	($\downarrow 99.2\%$)	($\downarrow 89.5\%$)	($\downarrow 94.1\%$)

TABLE II

TRAINING COMPUTATION COST COMPARISON ON OPV2V-H USING m_1 AS THE COLLABORATIVE BASE, SUMMED FOR NEW HETEROGENEOUS AGENTS (m_2, m_3, m_4). TT = TRAINING THROUGHPUT (SAMPLES/SEC.), TF = TFLOPS (TFLOPS/SEC.), AND PM = PEAK MEMORY USAGE.

Metric	TT \uparrow	TF \uparrow	PM (GB) \downarrow
HEAL [11]	26.12	13.94	7.0
FASTER-HEAL (ours)	30.44	16.63	4.3
Improvement	$\uparrow 1.16\times$	$\uparrow 1.19\times$	($\downarrow 38.6\%$)

TABLE III

ABLATION STUDY ON STAGE 2 TRAINING COMPONENTS FOR NEW AGENT ADAPTATION (m_2, m_3, m_4), WITH m_1 AS THE COLLABORATIVE BASE. WE COMPARE FREEZING OR TUNING THE ENCODER, BEV BACKBONE (BEV), AND LIFT. THE ALIGNER IS TRAINED IN ALL CASES.

Training Components	AP@0.5(%) \uparrow	AP@0.7(%) \uparrow	#TP (M) \downarrow
Encoder + BEV (HEAL)	90.9	84.5	18
Encoder + BEV + LIFT	89.6	83.1	18
Encoder + LIFT	92.2	85.3	17.2
BEV + LIFT	90.7	83.6	1.14
LIFT (ours)	92.7	85.7	0.34

TABLE IV

EFFECT OF DECOMPOSITION RANK R IN PARAFAC DECOMPOSITION ON NEW-AGENT ADAPTATION. WE REPORT DETECTION ACCURACY (AP@0.5, AP@0.7) AND THE NUMBER OF TRAINABLE PARAMETERS (#TP). RESULTS SHOW THAT $R = 8$ PROVIDES THE BEST TRADE-OFF THE RESULTS ARE REPORTED FOR $m_1 + m_2 + m_3 + m_4$.

R	AP@0.5(%) \uparrow	AP@0.7(%) \uparrow	#TP (M) \downarrow
4	91.6	84.0	0.335
8	92.7	85.7	0.340
16	89.7	82.1	0.352
32	91.4	84.0	0.373
64	90.2	83.0	0.416

- [10] R. Wang, H. Xiang, J. Li, R. Xu, Z. Tu. CoCMT: Towards Communication-Efficient Cross-Modal Transformer For Collaborative Perception, in Proceedings of the IEEE International Conference on Robotics and Automation (ICRA), 2024.
- [11] Y. Lu, Y. Hu, Y. Zhong, D. Wang, Y. Wang, S. Chen, An extensible framework for open heterogeneous collaborative perception. arXiv preprint arXiv:2401.13964, January 2024.
- [12] R. Xu, J. Li, X. Dong, H. Yu, and J. Ma. Bridging the domain gap for multi-agent perception. In 2023 IEEE International Conference on Robotics and Automation (ICRA), pages 6035–6042, 2023.
- [13] L. Xin, G. Zhou, Z. Yu, D. Wang, T. Luo, X. Fu, J. Li, PnPDA+: A Meta Feature-Guided Domain Adapter for Collaborative Perception. World Electric Vehicle Journal. January 2025.
- [14] Y. Xia, Q. Yuan, G. Luo, X. Fu, Y. Li, X. Zhu, et al., One is Plenty: A Polymorphic Feature Interpreter for Immutable Heterogeneous Collaborative Perception. In Proceedings of the Computer Vision and Pattern Recognition Conference 2025 (pp. 1592-1601).
- [15] M. Singha, H. Pal, A. Jha, and B. Banerjee. Ad-clip: Adapting domains in prompt space using clip. In 2023 IEEE/CVF International Conference on Computer Vision Workshops (ICCVW), pages 4357–4366, 2023.
- [16] M. Cai, H. Liu, S. K. Mustikovela, G. P. Meyer, Y. Chai, D. Park, and Y. J. Lee. Viplava: Making large multimodal models understand arbitrary visual prompts. In Proceedings of the IEEE/CVF Conference on Computer Vision and Pattern Recognition (CVPR), 2024.
- [17] D. Cheng, Z. Xu, X. Jiang, N. Wang, D. Li, and X. Gao. Disentangled prompt representation for domain generalization. In Proceedings of the IEEE/CVF Conference on Computer Vision and Pattern Recognition (CVPR), pages 23595–23604, 2024.
- [18] X. Zhang, F. Wei, Y. Wang, W. Zhao, F. Li, X. Chu. UPRE: Zero-Shot Domain Adaptation for Object Detection via Unified Prompt and Representation Enhancement. arXiv preprint arXiv:2507.00721, 2025.
- [19] H. R. Medeiros, A. Belal, S. Muralidharan, E. Granger, M. Pedersoli. Visual Modality Prompt for Adapting Vision-Language Object Detectors. arXiv preprint arXiv:2412.00622, 2024.
- [20] S. Xie, R. Girshick, P. Dollár, Z. Tu, and K. He. Aggregated residual transformations for deep neural networks. In Proceedings of the IEEE conference on computer vision and pattern recognition, 2017.
- [21] Z. Liu, H. Mao, C. YuanWu, C. Feichtenhofer, T. Darrell, and S. Xie. A convnet for the 2020s. In Proceedings of the IEEE/CVF Conference on Computer Vision and Pattern Recognition, pp. 11976–11986, 2022.
- [22] R. Xu, H. Xiang, X. Xia, X. Han, J. Li, and J. Ma. Opv2v: An open benchmark dataset and fusion pipeline for perception with vehicle-to-vehicle communication. In 2022 International Conference on Robotics and Automation (ICRA), pp. 2583–2589. IEEE, 2022.
- [23] A. H. Lang, S. Vora, H. Caesar, L. Zhou, J. Yang, and O. Beijbom. Pointpillars: Fast encoders for object detection from point clouds. In Proceedings of the IEEE/CVF conference on computer vision and pattern recognition, pp. 12697–12705, 2019.
- [24] Y. Yan, Y. Mao, and B. Li. Second: Sparsely embedded convolutional detection. Sensors, 18(10):3337, 2018.
- [25] M. Tan and Q. Le. Efficientnet: Rethinking model scaling for convolutional neural networks. In International conference on machine learning, pp. 6105–6114. PMLR, 2019.
- [26] K. He, X. Zhang, S. Ren, and J. Sun. Deep residual learning for image recognition. In Proceedings of the IEEE conference on computer vision and pattern recognition, pp. 770–778, 2016.
- [27] J. Philion and S. Fidler. Lift, splat, shoot: Encoding images from arbitrary camera rigs by implicitly unprojecting to 3d. In Computer Vision—ECCV 2020: 16th European Conference, Glasgow, UK, August 23–28, 2020, Proceedings, Part XIV 16, pp. 194–210. Springer, 2020.
- [28] R. Xu, Z. Tu, H. Xiang, W. Shao, B. Zhou, and J. Ma. Cobevt: Cooperative bird’s eye view semantic segmentation with sparse transformers. arXiv preprint arXiv:2207.02202, 2022.
- [29] J. D. Carroll, J. J. Chang. Analysis of individual differences in multidimensional scaling via an N-way generalization of “Eckart-Young” decomposition. Psychometrika. 1970 Sep;35(3):283-319.